iScience

CellPress
OPEN ACCESS

Article

Magnetically modulated photochemical reaction pathways in anthraquinone molecules and aggregates

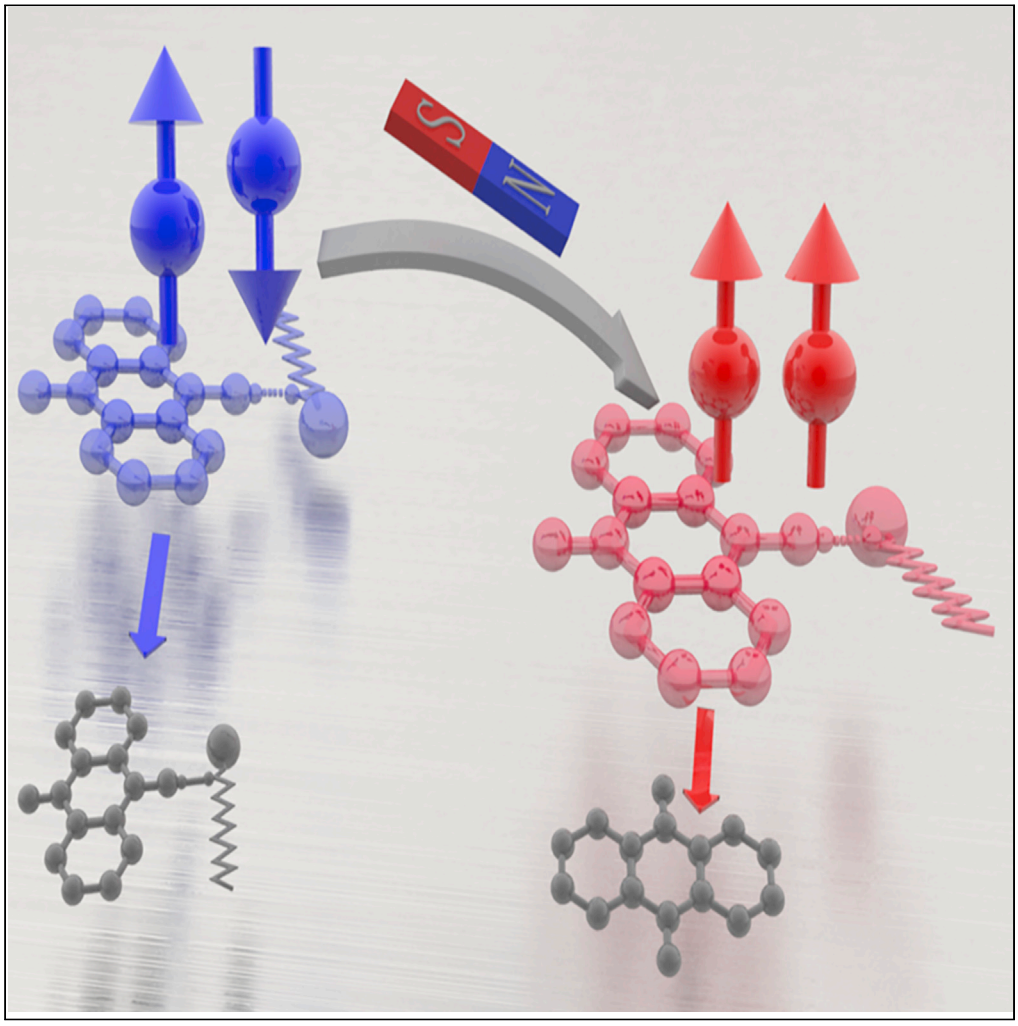

Wubin Wu, Baipeng Yin, Wei Peng, ..., Hua Sheng, Wanhong Ma, Chuang Zhang

zhangc@iccas.ac.cn

Highlights

Magnetically modulated photochemical reaction provides guidelines for organic synthesis

Magnetic field can facilitate the singlet-triplet spin conversion of radical pairs

Time-resolved spectroscopy reveals magnetically modulated dynamics of radical pairs

Wu et al., iScience 24, 102458
May 21, 2021
https://doi.org/10.1016/j.isci.2021.102458

iScience

CellPress
OPEN ACCESS

Article

Magnetically modulated photochemical reaction pathways in anthraquinone molecules and aggregates

Wubin Wu,[1,2] Baipeng Yin,[1,2] Wei Peng,[1,2] Yukun Zhao,[1,2] Zeyang Zhou,[1,2] Hua Sheng,[1,2] Wanhong Ma,[1,2] and Chuang Zhang[1,2,3,*]

SUMMARY

The chemical reactions involving excited-state radical pairs (RPs) of parallel/anti-parallel spin configurations are sensitive to magnetic field, leading to the possibilities of magnetically controlled synthesis of chemical compounds. Here we show that the reaction of anthraquinone (AQ) in sodium dodecyl sulfate (SDS) micellar solution under UV excitation is significantly influenced by applying external field. The steady state and time-resolved spectroscopies reveal that the reaction intermediate (pairs of AQH-SDS radicals) can undergo two distinct pathways depending on whether it is spin singlet or triplet, and the field is beneficial to the conversion between spin configurations of RPs. The applied field not only affects the reaction rate constant but also changes the final products. Besides, the aggregation of AQ molecules would change the population of singlets and triplets and thus enhance magnetic field effect. This work represents a promising way of controlling chemical reaction and improving reaction selectivity *via* magnetic field methods.

INTRODUCTION

The photochemical reactions have been encouraging the development of synthetic chemistry during past decades, as the excited-state molecules can undergo transformations that are significantly distinctive from those of ground state (Lang et al., 2014; Mou et al., 2019; Yang et al., 2020; Zhou and Zhang, 2020). In addition to the higher energy level than the ground state, the excited state usually has both singlet and triplet characteristics of spin1/2 pair (Miura et al., 2017), which allows for the observation of magnetic field effects (MFEs) on a series of photochemical systems (Buchachenko and Lawler, 2017; Chesta et al., 2007; Okazaki et al., 1996). Although previous reports have showed that applying magnetic field could modulate the rate and the yield of certain reactions such as photo-induced bond cleavage (Turro and Cherry, 1978; Tanimoto et al., 1984), the underlying mechanism is under debate and the quantitative studies are still missing (Binhi, 2002). We propose that the excited-state singlet and triplet may experience distinct reaction pathways; so the external field can affect photochemical reaction by altering spin configurations of excited state (Vink and Woodward, 2004).

When the energy difference between singlet and triplet, ΔE_{ST}, is sufficiently small (~μeV), the excited state becomes sensitive to relatively low field (~kG). Radical pairs (RPs), in which the spin1/2 radicals are located on weakly bounded molecules, have negligible ΔE_{ST} compared with those highly localized photo-generated excitons (Nagaoka et al., 2012; Xu et al., 2019; Yang et al., 2019). RPs with parallel and anti-parallel spin configurations may undergo distinct reaction pathways, which plays an important role in various types of chemical reactions. The conversion between spin configurations could naturally occur with the help of hyperfine interaction or spin-orbital coupling (Buchachenko, 2001.), and applying magnetic field would affect this spin-mixing process and consequently alter the ratio between parallel/anti-parallel spin configurations in RPs. This excited-state intermediate RPs is proved to be responsible for most MFEs in photochemical reactions (Dodson et al., 2015; Richert et al., 2013), which is similar to the polaron pairs that enable MFEs on charge recombination/dissociation in organic semiconductors (Hu and Wu, 2007; Sheng et al., 2014; Wang et al., 2019). Recent advances in organic spintronics reveal that steady-state and time-resolved spectroscopy techniques are powerful tools to investigate the spin state dynamics and the spin-dependent excited state processes (Zhang et al., 2015). It motivates our research on the spin-chemistry analogy using

[1]Key Laboratory of Photochemistry, Beijing National Laboratory for Molecular Sciences, Institute of Chemistry, Chinese Academy of Sciences, Beijing 100190, China

[2]University of Chinese Academy of Sciences, Beijing 100049, China

[3]Lead contact

*Correspondence: zhangc@iccas.ac.cn

https://doi.org/10.1016/j.isci.2021.102458

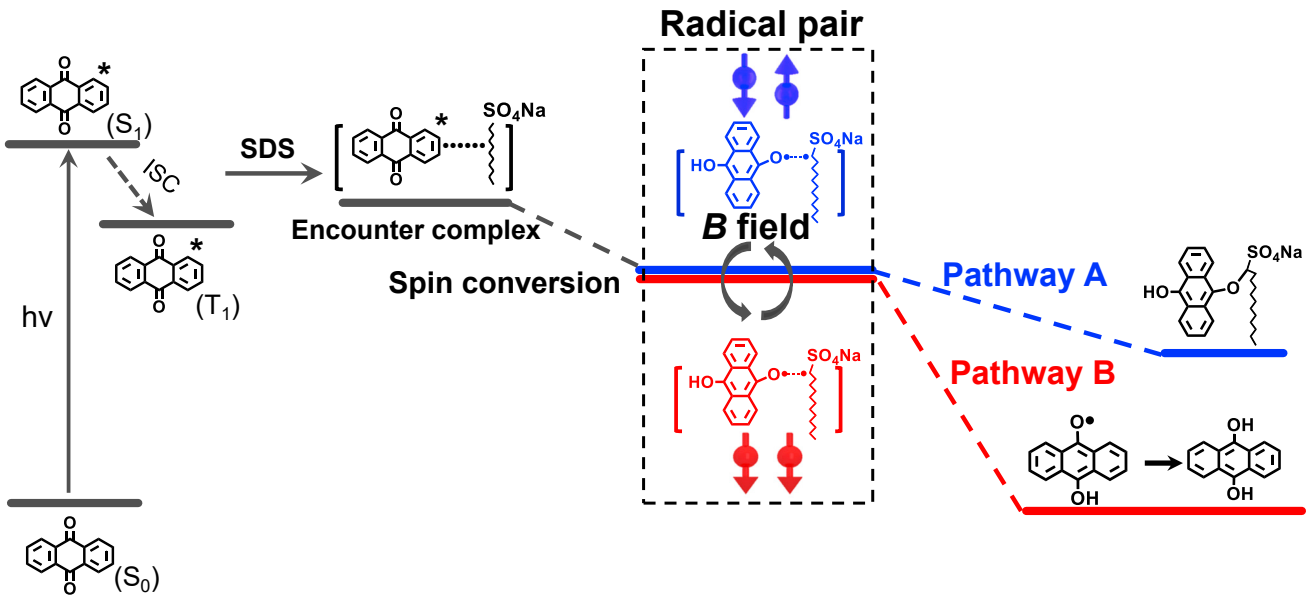

Scheme 1. Reaction pathways involving AQ-SDS radical pairs

Mechanism for MFEs on the photochemical reaction of AQ molecules in SDS micellar solution.

optical spectroscopy techniques under magnetic field, providing opportunities in exploring magnetically modulated reaction pathways toward highly efficient and selective photochemical synthesis under applied field (Kattnig and Hore, 2017).

In this work, magnetically modulated photochemical reaction pathways of anthraquinone (AQ) in the presence of sodium dodecyl sulfate (SDS) micellar solution were investigated systematically. Because molecular aggregates can cause quenching of singlet excitons and consequently affect the formation of singlets and triplets, we explored the role of AQ aggregates in magnified MFEs in magnetically modulated photochemical process. We quantified the magnitude of MFEs by using in situ absorption spectroscopy to monitor the process of photochemical reaction under external magnetic field. Interestingly, the applied field not only affects the reaction rate constant but also changes the final products, which was proved by high-performance liquid chromatography (HPLC) characterization. It was found that external field could facilitate the spin conversion of AQH-SDS RPs, in accordance with our transient absorption measurements on the excited state species of reaction intermediates. By monitoring the temporal evolution of AQH-SDS RPs, we demonstrated that the decay dynamics of spin states are essential to the observation of MFEs in these photochemical systems. Specifically, the formation of AQ aggregates in dilute SDS aqueous solution significantly increases the magnitude of MFEs, due to the aggregation caused quenching of singlet species as well as the prolonged lifetime of triplet photoexcitation. These results indicate the great potentials of magnetic field in controlling the reaction pathways and products of photochemical synthesis involving radical intermediates.

RESULTS AND DISCUSSION

Magnetic field effect on photochemical reaction pathways in micellar solution

The photobleaching of AQ molecules in SDS solution is a typical photochemical reaction which involves spin parallel and anti-parallel RPs and thus enables the existence of MFEs (Margulis et al., 1985), as illustrated in Scheme 1. AQ molecules are excited from their ground state under UV radiation to generate singlet excitons (S_1) while triplets (T_1) are also obtained via intersystem crossing (ISC). The coupling between AQ excitations and SDS molecules results in the encounter complex ([AQ*••••••SDS]) and consequently the pairs of AQ[+H]• and SDS[-H]• radicals (AQH-SDS RPs) upon the transfer of protons. The spin selection rule determines that these spin1/2 pairs of radicals have both parallel and anti-parallel configurations similar to singlet and triplet of AQ excitons. Nevertheless, the exchange interaction in delocalized RPs becomes much smaller than that of excitons, meaning that ΔE_{ST} is negligible. The conservation of energy can therefore be easily fulfilled for the spin conversion of AQH-SDS RPs at room temperature (thermal

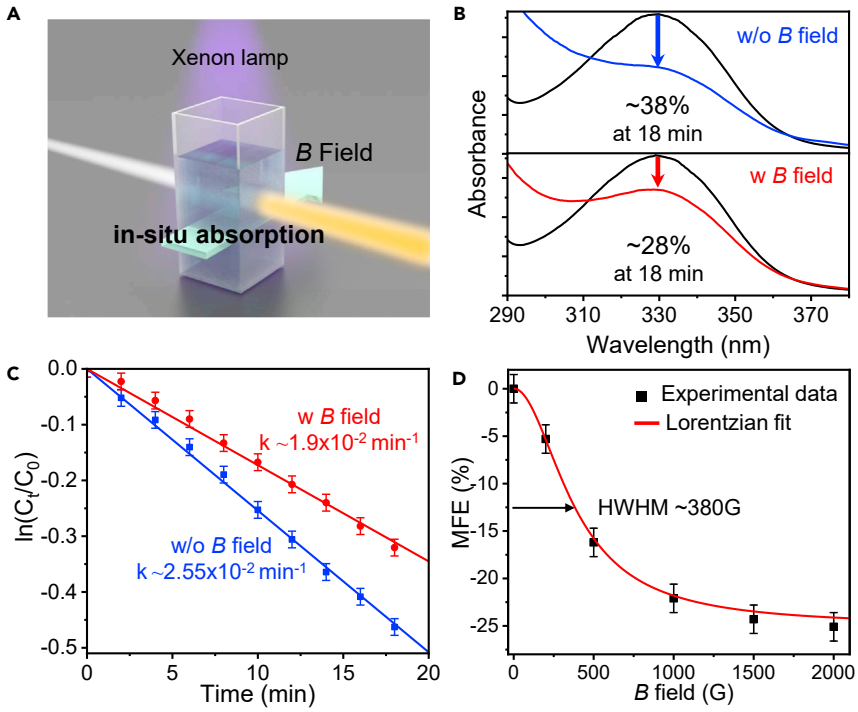

Figure 1. Magnetic field effect on AQ photobleaching reaction rate

(A) Illustration for in situ absorption measurement on photochemical reaction under magnetic field.

(B) Absorption spectra of AQ in SDS solution before (black)/after UV irradiation under zero (blue) or 2000 G (red) field.

(C) The change in AQ concentration versus the time of UV irradiation under zero (blue) or 2000 G (red) field. The initial concentrations of AQ and SDS are 0.4 mM and 0.4 M, respectively.

(D) MFEs magnitudes on the reaction rate of AQ in SDS solution at various B fields.

fluctuation ~25 meV), and the conservation of angular momentum becomes predominated in this spin mixing process. Applying external magnetic field can modulate the conversion between the singlet and triplet spin configurations in pair of radicals and change the singlet-to-triplet ratio of pair of radicals (Rodgers et al., 2007). It is thus possible to observe MFEs on the reaction (Frankevich et al., 1996), although the in-depth mechanism is not clear so far. Inspired by the polaron pair model for organic magnetoresistance (Hu et al., 2010), we propose that the reaction pathways should be spin-dependent, i.e., the AQH-SDS RPs undergo spin-dependent reaction pathways (pathway A and pathway B) that lead to distinct products (cage-type and escape-type) (Okazaki et al., 2002; Turro and Mattay, 1981). The difference between two pathways (A and B) is thereby responsible for the previously reported MFEs in terms of reaction rate (Misra et al., 1999)

We built an in situ absorption measurement setup (Figure 1A) to examine the change of AQ concentration upon the UV irradiation of Xenon lamp under applied magnetic field, B (Also see Figure S1 in supplemental information). As shown in Figure 1B, the absorption band of AQ at ~330 nm gradually decreases by ~38% after 18 min UV irradiation at zero field. Interestingly, the decrease in absorption intensity at 18 min is only ~28% when a B field of 2000 G (=0.2 Tesla) is applied on the cuvette, which indicates that the photochemical reaction of AQ molecules becomes less efficient under magnetic field (Scalano and Lougnot, 1984). Based on the Lambert-Beer law, the ratio between the concentration of AQ molecules C and its initial value C_0 is given by $C/C_0 = a/a_0$, where a_0 and a are the absorbance of sample solution before and after UV irradiation, respectively. Therefore, we can obtain the reaction kinetics with/without B field (Figure 1C), in which the reaction rate constant k is calculated by fitting the data points with the first-order reaction kinetic model (See calculations in supplemental information). It is obvious that the rate constant decreases from k_0~2.55 × 10^{-2} min^{-1} at zero field to k_B~1.9 × 10^{-2} min^{-1} at B = 2000 G, meaning that the photochemical reaction of AQ molecules is significantly slowed down by applying magnetic field (Tanimoto et al., 1983a, 1983b). The magnitude of MFEs is calculated by $(k_B - k_0)/k_0 \times 100\%$, and the MFEs on reaction rate at different field strengths are plotted in Figure 1D. The field dependence can be well fitted by a Lorentzian

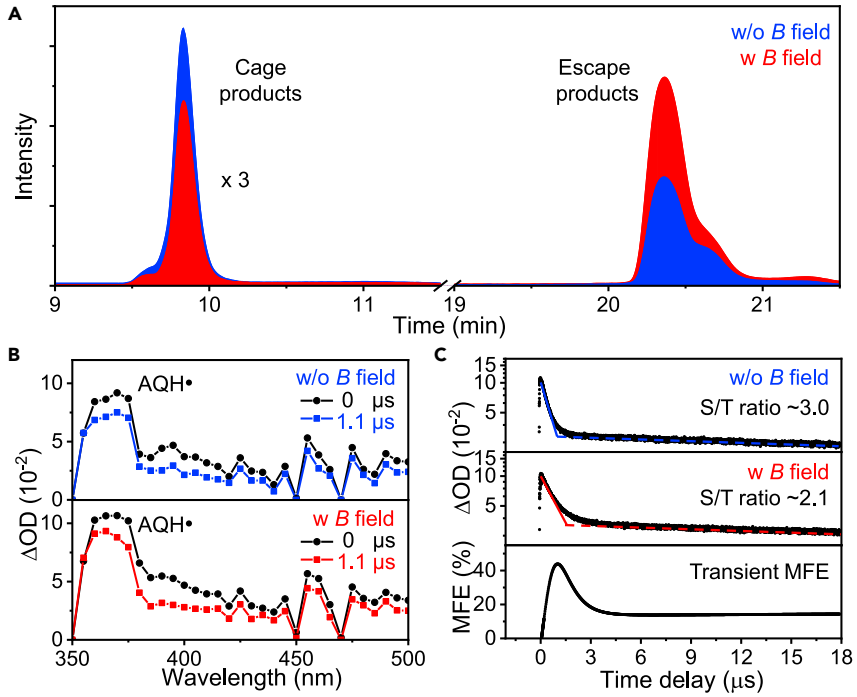

Figure 2. Magnetic field effect on reaction products and intermediates

(A) HPLC chromatogram of the AQ-SDS reaction products obtained under zero (blue) or 2000 G (red) field.

(B) Transient absorption spectra of AQ in SDS solution under zero (top) or 2000 G (bottom) field, pumped with a 355nm pulsed laser.

(C) Decay profiles of AQH• photoexcitation under zero (top) or 2000 G (middle) field, and the corresponding transient MFE (bottom).

function that saturates at nearly 25% with a half-width at half maximum (HWHM) of ~380 G, which is similar to the MFEs governed by spin-mixing via Δg mechanism observed in exciplex materials (Baniya et al., 2016). It should be mentioned that our measurements were carried out under ambient conditions, although the reaction rate, as well as the amplitude of MFE is dependent on that the solution temperature (Table S1) and the dissolved oxygen (Table S2).

Products analysis and temporal evolution of reaction intermediates

The change in reaction rate under magnetic field is caused by the modulation on the relative quantities of spin singlet/triplet RPs, which indicates that the two spin configurations should have different reaction rates. We speculate that the difference in reaction rates originates from the complexity of reaction pathways (Figure S2), which may also lead to MFEs on the reaction products. As shown in Figure 2A, we analyzed the products with/without B field by HPLC, which was not distinguishable from absorption spectra (Figure S3). Although the products of AQ photobleaching are quite complicated, they can be divided into two sets of compositions, i.e., the cage products (AQH-SDS) and escape products (anthrahydroquinone) (Tanimoto et al., 1983a, 1983b). The cage products are formed by recombination reaction of singlet RPs according to the Pauli principle, while escape products are generated by hydrogen abstraction of free radicals. The former one containing alkyl sulfate ion has stronger polarity similar to SDS amphiphile (Figure S4) and appears at a shorter retention time (~9.5 min) in HPLC. In comparison, the signal of escape product could be collected at a longer retention time (~20 min) which is close to that of raw AQ molecules (Figure S5). It was found that these two types of products (cage and escape) had different molar ratios for the reaction occurring with/without magnetic field, and more importantly, the field obviously improves the yield of escape product that is corresponding to the triplet RP intermediate (Feskov et al., 2019).

To directly observe the temporal evolution of AQH-SDS photoexcitation, time-resolved transient absorption was carried out using a nanosecond laser flash photolysis system, as shown in Figure 2B. The

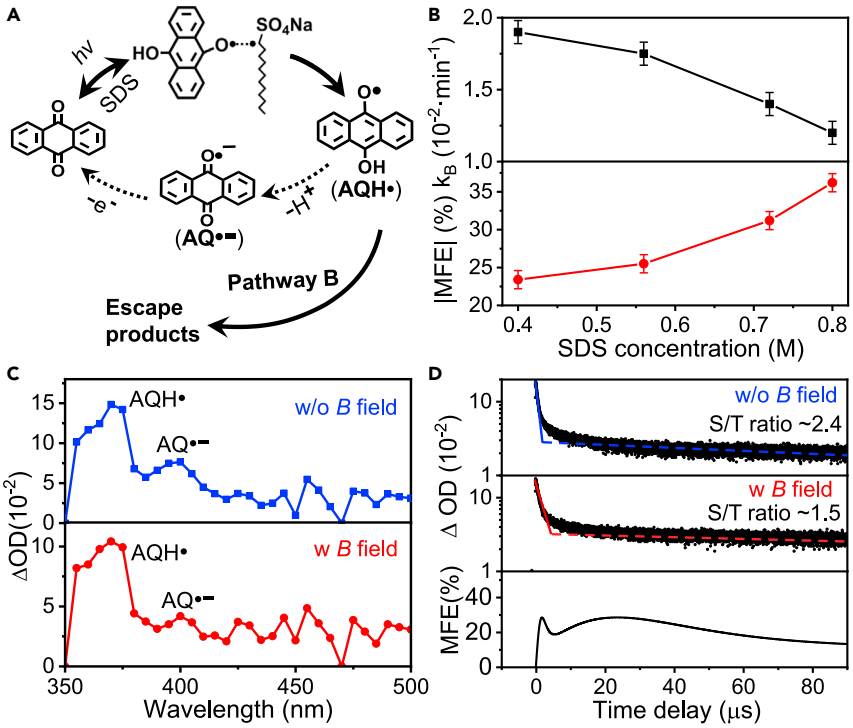

Figure 3. Magnetically modulated reaction pathway upon high initial SDS concentration

(A) Reaction cycle of AQ, AQ•- and AQH• in Pathway (B).

(B) Reaction rate constants at B = 2000 G and corresponding MFE magnitudes for the AQ reaction in SDS solutions with various concentrations (0.4–0.8 M).

(C) Transient absorption spectra of AQ in SDS solution (0.8 M) under zero (blue) or 2000 G (red) field.

(D) Decay profiles of AQH• photoexcitation under zero (top) or 2000 G (middle) field, and the corresponding transient MFE (bottom).

absorption band at 370 nm is attributed to the excited state absorption of AQH• radical that is a part of AQH-SDS RPs (Chowdhury and Basu, 2006). It is noted that the decay of AQH• radical becomes slower when magnetic field is applied. The decay profile of AQH• radicals (Figure 2C) can be fitted by a sum of two first-order decays (Zollitsch et al., 2018) (See Table S1 in supplemental information), in which the fast (solid line) and slow (dashed line) components are corresponding to AQH• radicals in the spin parallel and anti-parallel RPs, respectively. The weight ratio of fast/slow components is thus regarded as the ratio between singlet/triplet RPs (S/T ratio) in photochemical process. It was found that the S/T ratio decreased from 3 at zero field to 2.1 at B = 2000 G, meaning that the field facilitates the generation of spin triplet AQ-SDS RPs, which agrees with the increased yield of escape product. By analyzing the decay curves with/without field, we could also obtain a transient curve for the MFE on decay dynamics, which indicates that the conversion between two spin configurations almost completes within several microseconds.

Magnetically modulated dynamics of singlet and triplet radical pairs

The external field reduces the overall reaction rate of AQ photobleaching, as it promotes the reaction through pathway B (corresponding to spin triplet RPs) which has a relatively lower rate. In pathway B, the AQH• radicals undergo an escape process before forming the escape products (Haldar and Chowdhury, 1999), which includes the dissociation of RPs and the escape of AQH• radicals from SDS micellar cages. Thus, the concentration of SDS micelles becomes crucial for the reaction rate of pathway B and can consequently influence the observation of MFEs. As shown in Figure 3A, the formation of AQH-SDS intermediate between AQ and SDS molecules is reversible because of the weak coupling interaction of radicals. A part of AQH• radicals may dissociate into AQ•- anion radicals by losing protons and then go back to AQ molecules as semiquinone radicals are acidic (Sakaguchi and Hayashi, 1984). Increasing SDS concentration would limit the escape of AQH• radicals from micelles, and thus enhance the dissociation of AQH• into AQ•- anions. The rate constant of AQ photochemical reaction therefore decreases with the increase of

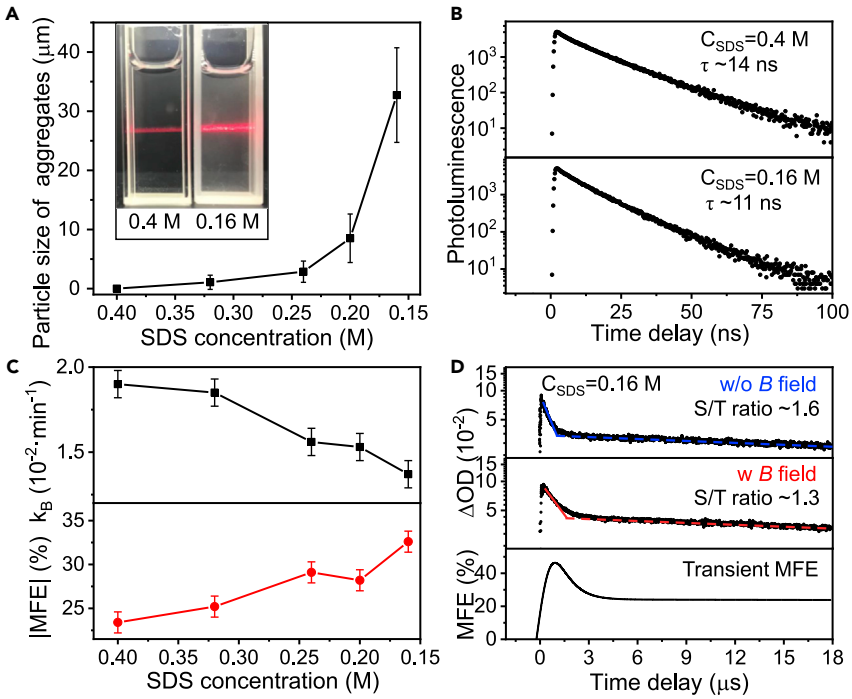

Figure 4. Magnetically modulated singlet and triplet radical pairs in AQ aggregates

(A) Average sizes of AQ aggregates obtained from low concentration SDS solutions (0.4–0.16 M). Inset: photograph of a laser beam passing through the AQ-SDS solutions.

(B) Decay profiles of photoluminescence at 450 nm from AQ molecules in SDS solutions (0.4 and 0.16 M).

(C) Reaction rate constants at B = 2000 G and the corresponding MFE magnitudes for the AQ reaction in SDS solutions with various concentrations (0.4–0.16 M).

(D) Decay profiles of AQH• photoexcitation under zero (top) or 2000 G (middle) field, and the corresponding transient MFE (bottom).

SDS concentration, as shown in Figure 3B. In comparison, the MFE magnitude has a significant increase from ~20% to ~35% with the increase of SDS concentration (Figure S6), while the field dependence curves remain the same Lorentzian line shape when the SDS concentration becomes higher (Figure S7). In the transient absorption spectrum (Figure 3C), an absorption band that is assigned to AQ•- radicals appears at 390 nm due to the enhancement of reaction process involving AQ•- radicals for high SDS concentration (0.8 M). As shown in Figure 3D, the S/T ratio decreases when the field is applied, and moreover, it is much smaller compared with that for standard SDS concentration (0.4 M). It indicates that more spin-parallel triplet RPs could be generated as their lifetime is prolonged (Table S3) for high SDS concentration, leading to more obvious difference between pathway A (singlet RPs) and pathway B (triplet RPs) and consequently larger MFE magnitudes. In addition, the curve of transient MFE reaches a maximum at ~20 μs and then starts to decrease. The long tail could be related to the reaction cycle of AQ•- radicals that has a timescale up to millisecond (Figure S8).

The AQ molecules would no longer exist as single molecules but form molecular aggregates ranging from ~1 to 100 μm (See dynamic light scattering results in Figure S9) when the SDS concentration is decreased below 0.40 M. As shown in Figure 4A, the suspension of AQ aggregates was still transparent although Tyndall effect was observed, and size of AQ aggregates increased with the decrease in SDS concentration. The aggregation-caused quenching effect shortens the lifetime of photo-generated singlet excitons (Huang et al., 2019) as indicated by the fluorescence decay curves for the standard and low SDS concentration samples (Figure 4B). This would lead to a decrease in the number of singlet RPs formed by singlet excitons, resulting in less contribution of pathway A in the photobleaching of AQ molecules. As a result, the reaction rate constant decreases when the aggregation of AQ molecules occurs in low concentration SDS solution, as shown in Figure 4C. Interestingly, MFE is obviously enhanced for these AQ aggregates, and the HWHM of Lorentzian line shape for field dependence also increases to

~400 G (Figure S10) possibly due to the distinct singlet-to-triplet conversion in molecular aggregates. Meanwhile, the S/T ratio obtained from transient absorption (Figure S11) is much smaller than that for AQ solutions, and decreases from ~1.6 to ~1.3 upon the applied B field (Figure 4D). It indicates that the formation of spin singlet pairs of radicals is reduced in AQ aggregates because of the aggregation-induced quenching of singlet excitons. The long-lived component significantly increases in transient MFE because the molecular aggregation retards the coupling between AQ photoexcitation and SDS molecules into spin singlet/triplet AQ-SDS RPs.

Conclusion

In conclusion, we have revealed the role of magnetic field in the control over reaction rate, intermediates, and products of AQ molecule photochemical reaction in SDS solution. It is found that the singlet and triplet pairs of spin 1/2 radicals undergo two distinct pathways to yield cage and escape products, respectively, and the external field promotes the conversion from singlet into triplet RPs. The molecular aggregation can decrease the formation of singlets in initial condition and thus enhance the MFEs. Our results offer in-depth understanding in the MFEs on chemical reactions and prove the possibilities of magnetically modulating the reaction efficiency and selectivity.

Limitations of the study

In our study, we have revealed the role of magnetic field in the control over reaction rate, intermediates, and products in a typical photochemical reaction process. These findings and methods would be further applied to various photochemical reactions. As the photobleaching is usually a homogeneous reaction, the exploration on magnetic field effects on the systems involving heterogeneous photocatalysts is still challenging. More effects would be focused on heterogeneous photocatalysis in future studies.

STAR★METHODS

Detailed methods are provided in the online version of this paper and include the following:

- KEY RESOURCES TABLE
- RESOURCE AVAILABILITY
  - Lead contact
  - Materials availability
  - Data and code availability
- METHOD DETAILS
  - Materials
  - Preparation of AQ-SDS aqueous solutions
  - Calculations on the reaction rates of AQ photobleaching
  - Characterizations
  - Home-built magneto-optical setup for in situ absorption spectroscopy

SUPPLEMENTAL INFORMATION

Supplemental information can be found online at https://doi.org/10.1016/j.isci.2021.102458.

ACKNOWLEDGMENTS

This work was financially supported by the National Natural Science Foundation of China (No. 21873105).

AUTHOR CONTRIBUTIONS

Chuang Zhang conceived the idea and supervised the project. Wubin Wu built the magneto-optical setup and conducted the steady-state and transient spectroscopic measurements. Wei Peng and Yukun Zhao contributed to the high-performance liquid chromatography experiments. Wubin Wu and Chuang Zhang analyzed the data and wrote the draft. All the authors discussed the results and commented on the manuscript.

DECLARATION OF INTERESTS

The authors declare no competing interests.

Received: January 20, 2021
Revised: April 1, 2021
Accepted: April 19, 2021
Published: May 21, 2021

REFERENCES

Baniya, S., Pang, Z.Y., Sun, D.L., Zhai, Y.X., Kwon, O., Choi, H., Choi, B., Lee, S., and Vardeny, Z.V. (2016). Magnetic field effect in organic light-emitting diodes based on electron donor-acceptor exciplex chromophores doped with fluorescent emitters. Adv. Funct. Mater. *26*, 6930–6937.

Binhi, V.N. (2002). In Magnetobiology: Underlying Physical Problems, H. Berg, ed. (San Diego Academic Press), p. 473.

Buchachenko, A.L. (2001). Magnetic isotope effect: Nuclear spin control of chemical reactions. J. Phys. Chem. A *105*, 9995–10011.

Buchachenko, A., and Lawler, R.G. (2017). New possibilities for magnetic control of chemical and biochemical reactions. Acc. Chem. Res. *50*, 877–884.

Chesta, C.A., Mohanty, J., Nau, W.M., Bhattacharjee, U., and Weiss, R.G. (2007). New insights into the mechanism of triplet radical-pair combinations. The persistent radical effect masks the distinction between in-cage and out-of-cage processes. J. Am. Chem. Soc. *129*, 5012–5022.

Chowdhury, A., and Basu, S. (2006). Interactions between 9,10-anthraquinone and aromatic amines in homogeneous and micellar media: a laser flash photolysis and magnetic field effect study. J. Lumin. *121*, 113–122.

Dodson, C.A., Wedge, C.J., Murakami, M., Maeda, K., Wallace, M.I., and Hore, P.J. (2015). Fluorescence-detected magnetic field effects on radical pair reactions from femtolitre volumes. Chem. Commun. *51*, 8023–8026.

Feskov, S.V., Rogozina, M.V., Ivanov, A.I., Aster, A., Koch, M., and Vauthey, E. (2019). Magnetic field effect on ion pair dynamics upon bimolecular photoinduced electron transfer in solution. J. Chem. Phys. *150*, 024501.

Frankevich, E., Zakhidov, A., Yoshino, K., Maruyama, Y., and Yakushi, K. (1996). Photoconductivity of poly(2,5-diheptyloxy-p-phenylene vinylene) in the air atmosphere: magnetic-field effect and mechanism of generation and recombination of charge carriers. Phys. Rev. B *53*, 4498.

Haldar, M., and Chowdhury, M. (1999). Magnetic-field effect on the micellar surface-bound benzophenone tetracarboxylic acid-sodium salt in aqueous cetyltrimethylammonium bromide medium. Chem. Phys. Lett. *312*, 432–439.

Hu, B., and Wu, Y. (2007). Tuning magnetoresistance between positive and negative values in organic semiconductors. Nat. Mater. *6*, 985–991.

Hu, B., Yan, L., and Shao, M. (2010). Magnetic-field effects in organic semiconducting materials and devices. Adv. Mater. *21*, 1500–1516.

Huang, Y., Xing, J., Gong, Q., Chen, L.C., Liu, G., Yao, C., Wang, Z., Zhang, H.L., Chen, Z., and Zhang, Q. (2019). Reducing aggregation caused quenching effect through co-assembly of PAH chromophores and molecular barriers. Nat. Commun. *10*, 169.

Kattnig, D.R., and Hore, P.J. (2017). The sensitivity of a radical pair compass magnetoreceptor can be significantly amplified by radical scavengers. Sci. Rep. *7*, 11640.

Lang, X., Ma, W., Chen, C., Ji, H., and Zhao, J. (2014). Selective aerobic oxidation mediated by TiO2 photocatalysis. Acc. Chem. Res. *47*, 355–363.

Margulis, L.A., Khudyakov, I.V., and Kuzmin, V.A. (1985). Magnetic field effects on radical recombination in a cage and in the bulk of a viscous solvent. Chem. Phys. Lett. *119*, 244–250.

Miura, T., Fujiwara, D., Akiyama, K., Horikoshi, T., Suzuki, S., Kozaki, M., Okada, K., and Ikoma, T. (2017). Magnetic control of the charge-separated state lifetime realized by covalent attachment of a platinum complex. J. Phys. Chem. Lett. *8*, 661–665.

Misra, A., Haldar, M., and Chowdhury, M. (1999). Inversion in the magnetic field effect of benzilketyl: SDS radical pair at high fields. Chem. Phys. Lett. *305*, 63–70.

Mou, F., Zhang, J., Wu, Z., Du, S., Zhang, Z., Xu, L., and Guan, J. (2019). Phototactic flocking of photochemical micromotors. iScience *19*, 415–424.

Nagaoka, Y., Chen, O., Wang, Z., and Cao, Y.C. (2012). Structural control of nanocrystal superlattices using organic guest molecules. J. Am. Chem. Soc. *134*, 2868–2871.

Okazaki, M., Tanimoto, Y., Konishi, Y., and Toriyama, K. (1996). Control of photoreaction by ESR transition of the intermediate radical pair as evaluated by liquid chromatography. J. Phys. Chem. *100*, 9403–9406.

Okazaki, M., Toriyama, K., Oda, K., and Kasai, T. (2002). Mechanism of the magnetic field dependence for the liquid phase photoreaction in nanotube of MCM-41. Phys. Chem. Chem. Phys. *4*, 1201–1205.

Richert, S., Rosspeintner, A., Landgraf, S., Grampp, G., Vauthey, E., and Kattnig, D.R. (2013). Time-resolved magnetic field effects distinguish loose ion pairs from exciplexes. J. Am. Chem. Soc. *135*, 15144–15152.

Rodgers, C.T., Norman, S.A., Henbest, K.B., Timmel, C.R., and Hore, P.J. (2007). Determination of radical re-encounter probability distributions from magnetic field effects on reaction yields. J. Am. Chem. Soc. *129*, 6746–6755.

Sakaguchi, Y., and Hayashi, H. (1984). Laser-photolysis study of the photochemical reactions of naphthoquinones in a sodium dodecyl sulfate micelle under high magnetic fields. J. Phys. Chem. *88*, 1437–1440.

Scalano, J.C., and Lougnot, D.J. (1984). Magnetic field effects on the behaviour of carbene-derived radical pairs in microemulsions. Examination of carbene multiplicities. Chem. Phys. Lett. *105*, 535–538.

Sheng, Z.G., Nakamura, M., Koshibae, W., Makino, T., Tokura, Y., and Kawasaki, M. (2014). Magneto-tunable photocurrent in manganite-based heterojunctions. Nat. Commun. *5*, 4584.

Tanimoto, Y., Udagawa, H., Katsuda, Y., and Itoh, M. (1983a). Magnetic-field effects on the photolysis of para-benzoquinone derivatives in sodium dodecyl-sulfate micelles. J. Phys. Chem. *87*, 3976–3982.

Tanimoto, Y., Udagawa, H., and Itoh, M. (1983b). Magnetic field effects on the primary photochemical processes of anthraquinones in SDS micelles. J. Phys. Chem. *87*, 724–726.

Tanimoto, T.Y., Shimizu, K., and Itoh, M. (1984). Magnetic-field effect on the photosensitized oxidation reaction of 1,3-diphenylisobenzofuran in SDS micellar solutions. J. Am. Chem. Soc. *106*, 7257–7258.

Turro, N.J., and Cherry, W.R. (1978). Photoreactions in detergent solutions. enhancement of regioselectivity resulting from reduced dimensionality of substrates sequestered in a micelle. J. Am. Chem. Soc. *100*, 7431–7432.

Turro, N.J., and Mattay, J. (1981). Photochemistry of some deoxybenzoins in micellar solutions. Cage effects, isotope effects, and magnetic field effects. J. Am. Chem. Soc. *103*, 4200–4204.

Vink, C.B., and Woodward, J.R. (2004). Effect of a weak magnetic field on the reaction between neutral free radicals in isotropic solution. J. Am. Chem. Soc. *126*, 16730–16731.

Wang, J., Zhang, C., Liu, H., McLaughlin, R., Zhai, Y., Vardeny, S.R., Liu, X., McGill, S., Semenov, D., Guo, H., et al. (2019). Spin-optoelectronic devices based on hybrid organic-inorganic trihalide perovskites. Nat. Commun. *10*, 129.

Xu, Y., Liang, X., Zhou, X., Yuan, P., Zhou, J., Wang, C., Li, B., Hu, D., Qiao, X., Jiang, X.,

et al. (2019). Highly efficient blue fluorescent OLEDs based on upper level triplet-singlet intersystem crossing. Adv. Mater. *31*, 1807388.

Yang, X.L., Guo, J.D., Xiao, H., Feng, K., Chen, B., Tung, C.H., and Wu, L.Z. (2020). Photoredox catalysis of aromatic β-ketoesters for in situ production of transient and persistent radicals for organic transformation. Angew. Chem. Int. Ed. *59*, 5365–5370.

Yang, Z., Jiang, Y., Zhang, W., Ding, Y., Jiang, Y., Yin, J., Zhang, P., and Luo, H. (2019). Solid-state, low-cost, and green synthesis and robust photochemical hydrogen evolution performance of ternary TiO_2/$MgTiO_3$/C Photocatalysts. iScience *14*, 15–26.

Zhang, C., Sun, D., Sheng, C.X., Zhai, Y.X., Mielczarek, K., Zakhidov, A., and Vardeny, Z.V. (2015). Magnetic field effects in hybrid perovskite devices. Nat. Phys. *11*, 427–434.

Zhou, C., and Zhang, T.R. (2020). Photocatalytic alkane production from fatty acid decarboxylation over hydrogenated catalyst. Sci. Bull. *65*, 870–871.

Zollitsch, T.M., Jarocha, L.E., Bialas, C., Henbest, K.B., Kodali, G., Dutton, P.L., Moser, C.C., Timmel, C.R., Hore, P.J., and Mackenzie, S.R. (2018). Magnetically sensitive radical photochemistry of non-natural flavoproteins. J. Am. Chem. Soc. *140*, 8705–8713.

STAR★METHODS

KEY RESOURCES TABLE

REAGENT or RESOURCE	SOURCE	IDENTIFIER
Chemicals, peptides, and recombinant proteins		
Anthraquinone	Beijing InnoChem Science & Technology Co., Ltd (Beijing, China)	CAS:84-65-1
Sodium dodecyl sulfate	Beijing InnoChem Science & Technology Co., Ltd (Beijing, China)	CAS:151-21-3
N, N-Dimethylaniline	Aladdin Chemistry Co., Ltd. (Shanghai, China)	CAS:121-69-7
Other		
Agilent 1200 series HPLC (with Agilent Zorbax SB-C_{18} column)	Agilent Technologies	https://www.agilent.com/en/products/liquid-chromatography
LP920-K laser flash photolysis	Edinburgh Instruments	https://www.edinst.com/products/lp920-upgrades/
ALV CGS-3	ALV-GmbH	https://www.alvgmbh.de/Products/goniometers/ALV_CGS3/alv_cgs3.html
Quantaurus-Tau C11367 serial fluorescence lifetime analysis	Hamamatsu Photonics	http://hamamatsu.com.cn/product/16744.html

RESOURCE AVAILABILITY

Lead contact

Further information and requests for resources and materials should be directed to and will be fulfilled by the lead contact, Chuang Zhang (zhangc@iccas.ac.cn).

Materials availability

This study did not generate new unique reagents.

Data and code availability

There is no data set or code associated with this work.

METHOD DETAILS

Materials

Anthraquinone (AQ) and sodium dodecyl sulfate (SDS) were purchased from Beijing InnoChem Science & Technology Co., Ltd (Beijing, China). N, N-Dimethylaniline (DMA) were purchased from Aladdin Chemistry Co., Ltd. (Shanghai, China) and used without further purification. High purity water was obtained from a Millipore Lab Water system.

Preparation of AQ-SDS aqueous solutions

The powders of AQ (0.04 mmol, 8.3 mg) and SDS (16 mmol, 4.6 g) were added into 20 mL high purity water, and the mixture was heated up to 80°C under vigorous stirring on a hot plate. After several hours, the clear solution of AQ (2 mM) and SDS (0.8 M) was obtained. To prepare aqueous solutions with various AQ/SDS ratios, 2 mL of the above mixed solution was injected into 8 mL of the pure SDS micelle solution under continuous stirring. The concentrations of AQ and SDS were controlled to be 0.04 mM and 0.16 to 0.8M, respectively. The aggregation of AQ molecules appeared when the concentration of SDS was below 0.4 M.

Calculations on the reaction rates of AQ photobleaching

In the photobleaching reaction, the reaction rate is described by the first-order reaction kinetic model, $-dC/dt = kC$, where k is the reaction rate constant, t is reaction time, and C is the concentration of AQ solution.

The integrated rate law in logarithmic expression is thus given by, $\ln(C/C_0) = -kt$, where C_0 is the initial value of C. According to the Lambert-Beer law, $A = \varepsilon CL$, where A is the absorbance of AQ solution, ε is the absorption coefficient of AQ solution, and L is the length of sample cell, the ratio between the concentration of AQ solution C and its initial value C_0 is given by $C/C_0 = A/A0$, where A_0 is the initial value of the absorbance of AQ solution. Thereby, we could plot $\ln(C/C_0)$ as a function of reaction time t and obtain the value of rate constant k by fitting the data points with a straight line.

Characterizations

In situ absorption spectra were measured using a home-built magneto-optical setup (Figure S1, also see below). Reaction products were analyzed on a HPLC system (Agilent 1200, detection wavelength ~330 nm) equipped with an Agilent Zorbax SB-C_{18} column, using a mobile phase of methanol/water (injection volume ~10 μL, volume ratio ~1:3, flow rate ~0.2 mL/min). Transient absorption spectra and kinetics were measured with a laser flash photolysis spectrometer (Edinburgh Instruments LP920-K), in which the excitation laser at 355 nm was provided by a frequency-tripled Nd:YAG laser system (Quantel Brilliant, ~10 ns pulse). Dynamic light scattering was performed on a goniometer-based light scattering system (ALV CGS-3) to measure the hydrodynamic radius and the size distribution. The fluorescence decay curves were obtained on a fluorescence lifetime spectrometer (Quantaurus-Tau C11367-31) with a 365 nm picosecond laser.

Home-built magneto-optical setup for in situ absorption spectroscopy

The sample cell was placed in a steady-state magnetic field that was provided by an electromagnet (East Changing, EM-1). A stable Xenon lamp (15 W, intensity fluctuation <1%) was used to activate the photobleaching process of AQ molecules in the solution. The broadband probe light (200–1100 nm, 20 μW) was provided by an ultra-stable UV-Vis-NIR light source (Ocean Optics, DH-mini, intensity fluctuation <0.2%). The transmission light was thus collected into a fiber spectrometer (Ocean Optics, Maya2000 pro). The UV-Vis spectra of sample were automatically recorded on a desktop several minutes during the AQ photobleaching process. The power of light irradiation on the sample cube (area ~1 cm^2) was ~20 uW from the unfocused xenon lamp with optical filters (the sample cube was placed 30 cm below the lamp). The solution temperature was constantly ~30°C. during the irradiation of xenon lamp.